Inorg. Chem. **2008**, *47*, 69–77

Synthesis and Structural Characterization of a New Vapochromic Pt(II) Complex Based on the 1-Terpyridyl-2,3,4,5,6-pentaphenylbenzene (TPPPB) Ligand

Pingwu Du, Jacob Schneider, William W. Brennessel, and Richard Eisenberg*

Department of Chemistry, University of Rochester, Rochester, New York 14627

Received May 16, 2007

A novel terpyridine ligand containing a pentaphenylphenyl moiety linked to the terpyridyl core (1-terpyridyl-2,3,4,5,6-pentaphenyl-benzene (TPPPB)) has been synthesized in good yield and reacted with $Pt(DMSO)_2Cl_2$, to produce the cationic complex [Pt(TPPPB)Cl]Cl (**5**). **5** was studied structurally and spectroscopically. It is observed to be brightly luminescent in the solid state at room temperature and at 77 K, with no change in λ_{em}^{max}. The complex exhibits reversible vapochromic behavior upon exposure to methylene chloride vapors, changing color from red (**5-R**) to green (**5-G**). The shift to higher energy in the emission maximum from 654 to 514 nm is the largest vapochromic shift (140 nm) yet reported. The [Pt(TPPPB)Cl]Cl complex exhibits high selectivity for certain volatile organic compounds (VOCs) including methylene chloride, ethanol, ethyl acetate, and acetonitrile. The crystal structures of both the green and red forms have been determined by single-crystal X-ray diffraction. In both forms, the cationic Pt(II) complex possesses the anticipated square-planar coordination geometry that is distorted as a consequence of constraints from the terpyridyl binding. Analysis of the crystal packing of the green form (**5-G**) reveals the presence of non-interacting Pt···Pt separations with distances of 3.9092(9) and 4.5483(11) Å and a zigzag arrangement between neighboring Pt(II) ions. The red form (**5-R**) contains complexes that are stacked with Pt···Pt separations of 3.2981(14) and 3.3427(14) Å, indicative of metallophilic interaction. The change in the emitting state, as a consequence of the effect of the volatile organic compounds, results from a disruption of the d^8–d^8 metallophilic interactions in the red form and its metal–metal-to-ligand charge transfer (MMLCT) excited state to a more-localized Pt($d\pi$)-to-tpy(π^*) metal-to-ligand charge transfer (MLCT) excited state in the green form.

Introduction

The spontaneous formation of molecules into noncovalently bonded, well-defined, stable structures induced by self-assembly plays an important role in biological systems and has attracted increasing attention in the past two decades.[1−3] Among the variety of the noncovalent interactions that influence self-assembly, hydrogen bonding, $\pi-\pi$ interactions, and hydrophobic−hydrophobic interactions dominate the conformational dynamics of macromolecules such as proteins and nucleic acids, resulting in protein folding and the secondary and tertiary structure of nucleic acids.[4−8] In organometallic and metal complex chemistry, metallophilic bonding has also been explored as a noncovalent structure influencing interaction in platinum complexes,[9−18]

* To whom correspondence should be addressed. Email: eisenberg@chem.rochester.edu.

(1) Whitesides, G. M.; Grzyboski, B. *Science* **2002**, *295*, 2418−2421.
(2) Lehn, J.-M. *Supramolecular Chemistry Concepts and Perspectives*; VCH: Weinheim, Germany, 1995.
(3) Chambron, J.-C.; Dietrich-Buchecker, C.; Sauvage, J. *Transition Metals as Assembling and Templating Species: Synthesis of Catenanes and Molecular Knots. In Comprehensive Supramolecular Chemsitry*; Lehn, Jean-Marie; Atwood, J. L., Davies, J. E. D., MacNicol, D. D., Vögtle, F., Eds.; Pergamon Press: Oxford, U.K., 1996.
(4) Serrano, L.; Bycroft, M.; Fersht, A. R. *J. Mol. Biol.* **1991**, *218*, 465−475.
(5) Hunter, C. A.; Singh, J.; Thomton, J. M. *J. Mol. Biol.* **1991**, *218*, 837−846.
(6) Burley, S. K.; Petsko, G. A. *Science* **1985**, *229*, 23−28.
(7) Guckian, K. M.; Schweitzer, B. A.; Ren, R. X.-F.; Sheils, C. J.; Tahmassebi, D. C.; Kool, E. T. *J. Am. Chem. Soc.* **2000**, *122*, 2213−2222.
(8) Müller-Dethlefs, K.; Hobza, P. *Chem. Rev.* **2000**, *100*, 143−168.
(9) Houlding, V. H.; Miskowski, V. M. *Coord. Chem. Rev.* **1991**, *111*, 145−152.
(10) Chan, C.-W.; Cheng, L.-K.; Che, C.-M. *Coord. Chem. Rev.* **1994**, *132*, 87−97.
(11) Connick, W. B.; Geiger, D. P.; Eisenberg, R. *Inorg. Chem.* **1999**, *38*, 3264−3265.
(12) Yip, H. K.; Cheng, L. K.; Cheung, K. K.; Che, C. M. *J. Chem. Soc., Dalton Trans.* **1993**, 2933−2938.

10.1021/ic700947g CCC: $40.75
Published on Web 12/05/2007

rhodium complexes,[19−23] and silver, gold, and copper systems.[24−31] These complexes possess a rich range of spectroscopic and photophysical properties influenced by these metal−metal interactions, including photoluminescence properties in the solid state and even in fluid solution.[32−34]

Recently, a number of four-coordinate planar Pt(II) systems and linearly coordinated Au(I) complexes have been found to respond to different volatile organic compounds (VOCs) with changes in emission energies in fast real time, opening up interest in these systems for sensor applications.[35−37] For the Pt(II) complexes as solid samples, the VOC selectivity and emission energy changes have been postulated to result from changes in Pt···Pt interactions in the solid state, and in one case, this has been demonstrated by crystallographic characterization of the same crystal before and after exposure to MeOH vapors.[38] Only one example reveals a reversible change of molecular structure from $[PtClC_6H_2(CH_2NMe_2)_2$-2,6-OH] to $[PtClC_6H_2(CH_2NMe_2)_2$-SO_2-2,6-OH] upon exposure to SO_2.[39]

The architectures for Pt(II) complexes with vapochromic properties can be classified into four different types: (1) Pt(II) double salts with stacks of alternating cations and anions exhibiting metallophilic Pt···Pt interactions, (2) neutral Pt(II) complexes with crystal packing that indicate Pt···Pt interactions, (3) Pt(II) cationic complexes with simple anions that also show stacking of the planar complexes with Pt··· Pt interactions, and (4) isolated binuclear complexes that allow the stacking of planar platinum moieties and metallophilic interaction. For (1), the double salts of $[Pt(CNR)_4]$-$[M(CN)_4]$ (R= $C_{12}H_{25}$, $C_{14}H_{29}$; M = Pt, Pd) reported by Mann and co-workers consist of stacks of alternating $[Pt(CNR)_4]^{2+}$ cations and $[M(CN)_4]^{2-}$ anions in which d^8-d^8 interactions affect the luminescence reversibly when VOCs sorb into, and desorb from, voids between the stacks.[40,41] Examples of (2) are obtained when $[Pt(CNR)_4][Pt(CN)_4]$ systems are heated, leading to ligand-exchanged neutral complexes.[42] For one such system, *cis*-Pt(CN-*p*-(C_2H_5)-$C_6H_4)_2(CN)_2$, Mann and co-workers found that an orange morph exhibiting Pt···Pt interactions possesses vapochromic and vapoluminescent sensitivity to gaseous-phase aromatic hydrocarbons including benzene, toluene, and *p*-xylene that influence the Pt···Pt separation. For an example of case (3), Connick et al.[43] synthesized and studied the cationic complex [Pt(Me$_2$bzimpy)Cl]X (Me$_2$bzimpy = 2,6-bis-(*N*-methylbenzimidazol-2-yl)pyridine; X = Cl, PF_6), which gave a significant color change (e.g., from orange-red to yellow) upon exposure to selected VOCs (MeOH and CH_3CN). In a different study, Wadas et al.[38] reported the dicationic complex $[Pt(Nttpy)Cl](PF_6)_2$ (Nttpy = 4′-(*p*-nicotinamide-*N*-methylphenyl-2,2′:6′,2″-terpyridine) that showed a change in absorption and emission energies upon exposure to methanol and acetonitrile vapors. The structures of both forms were determined from the same crystal before and after exposure to MeOH vapor, confirming the change in Pt···Pt separations as key to the spectroscopic changes. A case of (4) can be found in the recent report by Che et al.,[44] who describe binuclear Pt(II) systems $[(R\text{-}C\hat{}N\hat{}C)_2Pt_2(\mu\text{-dppm})]$ (R= H, Ph, BrC_6H_5, 3,5-$F_2C_6H_3$) that have intramolecular Pt···Pt interactions with distances on the order of 3.3 Å. Upon diffusion of chloroform into one of these samples in the solid state, its color changed from red to yellow.

The present article reports the synthesis, structural characterization, and solid-state photophysical properties of a novel Pt(II) terpyridine complex that displays a selective and reversible vapochromic response toward a limited number of organic solvents. Distinctive features of the present system relative to those reported in previous studies on vapochromic behavior are a fast response to methylene chloride, high selectivity, a broad shift in emission color from red to green, and excellent stability at different temperatures. The X-ray

(13) Aldridge, T. K.; Stacy, E. M.; McMillin, D. R. *Inorg. Chem.* **1994**, *33*, 722−727.
(14) Arena, G.; Calogero, G.; Campagna, S.; Scolaro, L. M.; Ricevuto, V.; Romeo, R. *Inorg. Chem.* **1998**, *37*, 2763−2769.
(15) Cheung, T.-C.; Cheung, K.-K.; Peng, S.-M.; Che, C. M. *J. Chem. Soc., Dalton Trans.* **1996**, 1645−1651.
(16) Lai, S.-W.; Chan, M. C. W.; Cheung, K. K.; Che, C. M. *Organometallics* **1999**, *18*, 3327−3336.
(17) Lai, S.-W.; Chan, M. C. W.; Cheung, K.-K.; Che, C.-M. *Inorg. Chem.* **1999**, *38*, 4262−4267.
(18) Lai, S.-W.; Chan, M. C. W.; Cheung, K.-K.; Peng, S. M.; Che, C.-M. *Inorg. Chem.* **1999**, *38*, 4046−4055.
(19) Dallinger, R. F.; Miskowski, V. M.; Gray, H. B.; Woodruff, W. H. *J. Am. Chem. Soc.* **1981**, *103* (6), 1595−1596.
(20) Rice, S. F.; Gray, H. B. *J. Am. Chem. Soc.* **1981**, *103* (6), 1593−1595.
(21) Sigal, I. S.; Man, K. R.; Gray, H. B. *J. Am. Chem. Soc.* **1980**, *102* (24), 7252−7256.
(22) Esswein, A. J.; Veige, A. S.; Nocera, D. G. *J. Am. Chem. Soc.* **2005**, *12* (47), 16641−16651.
(23) Dempsey, J. L.; Esswein, A. J.; Manke, D. R.; Rosenthal, J.; Soper, J. D.; Nocera, A. G. *Inorg. Chem.* **2005**, *44* (20), 6879−6892.
(24) Schmidbaur, H. *Chem. Soc. Rev.* **1995**, *24*, 391−400.
(25) Pyykkö, P. *Chem. Rev.* **1997**, *97*, 597−636.
(26) White-Morris, R. L.; Olmstead, M. M.; Jiang, F.; Balch, A. L. *Inorg. Chem.* **2002**, *41* (9), 2313−2315.
(27) White-Morris, R. L.; Olmstead, M. M.; Balch, A. L. *J. Am. Chem. Soc.* **2003**, *125* (4), 1033−1040.
(28) Hayashi, A.; Olmstead, M. M.; Attar, S.; Balch, A. L. *J. Am. Chem. Soc.* **2002**, *124* (20), 5791−5795.
(29) Enomoto, M.; Kishimura, A.; Aida, T. *J. Am. Chem. Soc.* **2001**, *123*, 5608−5609.
(30) Wang, Q.-M. L., Y.-A.; Crespo, O.; Deaton, J.; Tang, C.; Gysling, H. J.; Concepcion Gimeno, M.; Larraz, C.; Villacampa, M. D.; Laguna, A.; Eisenberg, R. *J. Am. Chem. Soc.* **2004**, *126* (31), 9488−9489.
(31) Lee, Y.; Eisenberg, R. *J. Am. Chem. Soc.* **2003**, *125* (26), 7778−7779.
(32) Lai, S.-W.; Lam, H.-W.; Lu, W.; Cheung, K.-K.; Che, C. M. *Organometallics* **2002**, *21*, 226−234.
(33) Lu, W. C., M. C. W.; Zhu, N.; Che, C.-M.; Li, C.; Hui, Z. *J. Am. Chem. Soc.* **2004**, *126*, 7639−7651.
(34) Yam, V. W.-W.; Wong, K. M.-C.; Zhu, N. *J. Am. Chem. Soc.* **2002**, *124*, 6506−6507.
(35) Daws, C. A.; Exstrom, C. L.; Sowa, J. R., Jr.; Mann, K. R. *Chem. Mater.* **1997**, *9*, 363−368.
(36) Exstrom, C. L.; Sowa, J. R., Jr.; Daws, C. A.; Janzen, D.; Mann, K. R.; Moore, G. A.; Stewart, F. F. *Chem. Mater.* **1995**, *7*, 15−17.
(37) Fernandez, E. J.; Lopez-de-Luzuriaga, J. M.; Monge, M.; Olmos, M. E.; Perez, J.; Laguna, A.; Mohamed, A. A.; Fackler, J. P., Jr. *J. Am. Chem. Soc.* **2003**, *125*, 2022−2023.
(38) Wadas, T. J.; Wang, Q.-M.; Kim, Y.-j.; Flaschenreim, C.; N., B. T.; Eisenberg, R. *J. Am. Chem. Soc.* **2004**, *126*, 16841−16849.
(39) Albrecht, M.; Lutz, M.; Spek, A. L.; Van, Koten, G. *Nature* **2000**, *406*, 970−974.
(40) Drew, S. M. J., D. E.; Buss, C. E.; MacEwan, D. I.; Dublin, K. M.; Mann, K. R. *J. Am. Chem. Soc.* **2001**, *123* (34), 8414−8415.
(41) Exstrom, C. L.; Pomije, M. K.; Mann, K. R. *Chem. Mater.* **1998**, *10*, 942−945.
(42) Buss, C. E. M., K. R. *J. Am. Chem. Soc.* **2002**, *124* (6), 1031−1039.
(43) Grove, L. J.; Rennekamp, J. M.; Jude, H.; Connick, W. B. *J. Am. Chem. Soc.* **2004**, *126*, 1594−1595.
(44) Kui, S. C. F. C., S. S.-Y.; Che, C.-M.; Zhu, N. *J. Am. Chem. Soc.* **2006**, *128* (25), 8297−8309.

structural characterization of both the red and green forms of the title complex provide interesting details on the basis of the vapochromic effect in this system. The results show that the crystalline state possesses significant flexibility to allow expansion and contraction of the lattice with resultant slippage between neighboring stacked planar complexes that affects the metallophilic interactions between them and consequent emission behavior.

Experimental Section

Characterization. ^{1}H NMR (400.1 MHz) and ^{13}C NMR (75 MHz) spectra were recorded on a Bruker Avance-400 spectrometer. Mass determinations were carried out by electrospray ionization mass spectrometry (ESI-MS) using a Hewlett-Packard Series 1100 mass spectrometer (Model A) equipped with a quadrupole mass filter. Absorption spectra were recorded using a Hitachi U2000 scanning spectrophotometer (200−1100 nm), and elemental analyses were determined by Desert Analytics.

Luminescence. Luminescence spectra were obtained using a Spex Fluoromax-P fluorimeter corrected for the spectral sensitivity of the photomultiplier tube and the spectral output of the lamp with monochromators positioned for a 2 nm band-pass. Solution samples were degassed by three freeze−pump−thaw cycles, and frozen glass samples (1:4 (v/v) MeOH:EtOH) were prepared in NMR tubes placed in a quartz-tipped immersion dewar filled with liquid nitrogen. Solid-state emission samples were prepared as a 4% mixture (w/w) of the red form of [Pt(TPPPB)Cl]Cl in a matrix of finely ground KBr contained in resealable J. Young tubes and purged with argon. Solvent vapors for vapochromism studies were generated by vigorously bubbling argon through a sealed 100 mL Erlenmeyer flask containing the anhydrous solvent, and the vapors were transferred to the sample tube via cannula. Total exposure time of the sample to different VOC vapors was 30 min, and the removal of the vapors was accomplished by exposing the sample to the air or gently heating the sample under vacuum.

Syntheses of New Compounds 4-(Phenylethynyl)-2,2′:6′,2″-Terpyridine (2). A solution of 4′-[[(trifluoromethyl)sulfonyl]oxy]-2,2′:6′,2″-terpyridine[45] (0.5 g, 1.31 mmol), $Pd(PPh_3)_4$ (0.75 g, 0.065 mmol), and phenylacetylene (0.17 g, 1.62 mmol) in toluene (10 mL) containing triethylamine (15 mL) was heated at 100 °C for 24 h under a dry dinitrogen atmosphere. The solution was allowed to cool to room temperature, followed by the removal of the organic solvents under reduced pressure. The crude product was recrystallized from methanol, yielding an off-white solid (0.33 g, 74%). ^{1}H NMR (DMSO-d_6): δ 8.78−8.72 (2H, d), 8.70−8.60 (2H, d), 8.50 (2H, s), 8.10−8.00 (2H, t), 7.70−7.65 (2H, m), 7.60−7.45 (5H, m). ESI-MS calcd for M^+ 333.1, found 334.1 (MH^+).

1-Terpyridyl-2,3,4,5,6-pentaphenyl-benzene (TPPPB, 4). 4-(Phenylethynyl)-2,2′:6′,2″-terpyridine (0.20 g, 0.60mmol) and tetraphenylcyclopentadienone (0.23 mg, 0.60mmol) were heated to reflux in diphenyl ether (3 g) overnight. The dark-red solution was evaporated under reduced pressure. The crude product was washed by methanol to give an off-white solid (0.30 g, 69%). ^{1}H NMR (DMSO-d_6): δ 8.63−8.60 (2H, d), 8.38−8.35 (2H, d), 8.00 (2H, s), 7.88−7.84 (2H, t), 7.41−7.37 (2H, m), 7.00−6.75 (23H, m), 6.72−6.68 (2H, m). ^{13}C NMR (DMSO-d_6) at 25 °C: δ 156.1, 153.7, 150.0, 140.9, 140.5, 140.3, 140.0, 139.8, 136.4, 131.3, 131.2, 126.8, 126.6, 125.6, 125.3, 123.9, 123.3, 120.8. ESI-MS Calcd for M^+ 689.3, Found 690.3 (MH^+).

(45) Potts, K. T.; Konwar, D. *J. Org. Chem.* **1991**, *56*, 4815−4816.

[Pt(TPPPB)Cl]Cl (5). 1-Terpyridyl-2,3,4,5,6-pentaphenyl-benzene (TPPPB) (0.10 g, 0.15mmol) and $Pt(DMSO)_2Cl_2$ (0.061 g, 0.15mmol) were refluxed in 15 mL methanol for 24 h. The product precipitated from solution upon the addition of 15 mL diethyl ether and was isolated by filtration, followed by washing with cold ethanol and diethyl ether to yield a red solid denoted as **5-R** (0.116 g, yield, 75%). ^{1}H NMR (DMSO-d_6): 8.78−8.72 (2H, d), 8.70−8.60 (2H, d), 8.50 (2H,s), 8.10−8.00 (2H, t), 7.70−7.65 (2H, m), 7.60−7.45 (5H, m). ^{13}C NMR (DMSO-d_6) at 25 °C: δ 158.0, 155.8, 152.9, 152.0, 143.4, 142.6, 141.1, 139.7, 139.6, 139.4, 138.7, 136.6, 131.3, 131.0, 129.8, 127.8, 127.4, 127.3, 127.0, 126.9, 126.4, 125.5. ESI-MS calcd for M^+ 919.2, Found 920.2 (MH^+). Anal. Calcd ($C_{51}H_{35}Cl_2N_3Pt$): C, 64.09; H, 3.69; N, 4.40; Found: C. 63.96, H 3.85, N. 4.83.

Green crystals suitable for single-crystal X-ray diffraction were grown by the slow evaporation of a concentrated solution of **5** dissolved in methylene chloride at ambient temperature. The green form of **5** thus obtained is denoted as **5-G**. Anal. Calcd ($C_{51}H_{35}N_3Cl_2Pt{\cdot}CH_2Cl_2$): C, 60.01; H, 3.58; N, 4.04. Found: C, 60.13; H, 3.55; N, 4.09.

X-ray Structural Determinations of the Green (5-G) and Red (5-R) Forms of [Pt(TPPPB)Cl]Cl. A crystal of **5-G** ($0.50 \times 0.08 \times 0.02$ mm^3) was placed onto the tip of a 0.1 mm diameter glass capillary tube or fiber and mounted on a Bruker SMART APEX II CCD Platform diffractometer for data collection at 100.0(1) K. A preliminary set of cell constants and an orientation matrix were calculated from 296 reflections harvested from 3 sets of 20 frames. These initial sets of frames were oriented such that orthogonal wedges of reciprocal space were surveyed. Data collection was carried out using Mo Kα radiation (graphite monochromated) with a frame time of 90 s and a detector distance of 4.98 cm. Crystals of **5-G** undergo solvent loss at ambient temperature, with color changes from green to red (**5-R**), but the red crystals thus obtained were unsuitable for crystallography.

Crystals of **5-R** suitable for single-crystal X-ray diffraction were grown by the slow diffusion of diethyl ether into a concentrated solution of **5** dissolved in methanol at ambient temperature. A red crystal ($0.28 \times 0.12 \times 0.04$ mm^3) was placed onto the tip of a 0.1 mm diameter glass capillary tube or fiber and mounted on a Bruker SMART APEX II CCD Platform diffractometer for data collection at 100.0(1) K. A preliminary set of cell constants and an orientation matrix were calculated from 578 reflections harvested from 3 sets of 20 frames. These initial sets of frames were oriented such that orthogonal wedges of reciprocal space were surveyed.

The space groups were assigned as *C*2/*c* and *P*2/*n* for **5-G** and **5-R**, respectively. Both structures were solved by direct methods and refined employing full-matrix least-squares on F^2 (Bruker-AXS, *SHELXTL-NT*, version 5.10). For **5-G**, all of the non-hydrogen atoms were refined with anisotropic displacement parameters. All of the hydrogen atoms were placed in ideal positions and refined as riding atoms with relative isotropic displacement parameters. Reflection contributions from highly disordered solvent molecules (methanol and/or dichloromethane) were removed using program *PLATON*, function *SQUEEZE*, which determined there to be 812 electrons in a volume of 3099 Å removed. The final full-matrix least-squares refinement converged to $R1 = 0.0557$ (F^2, $I > 2\sigma(I)$) and $wR2 = 0.1268$ (F^2, all data).

For **5-R**, only the platinum and chlorine atoms were refined with anisotropic displacement parameters; all of the other atoms were refined with isotropic displacement parameters. All of the hydrogen atoms were placed in idealized positions and refined as riding atoms with relative isotropic displacement parameters. The final full-matrix least-squares refinement converged to $R1 = 0.1026$ (F^2, $I >$

Scheme 1

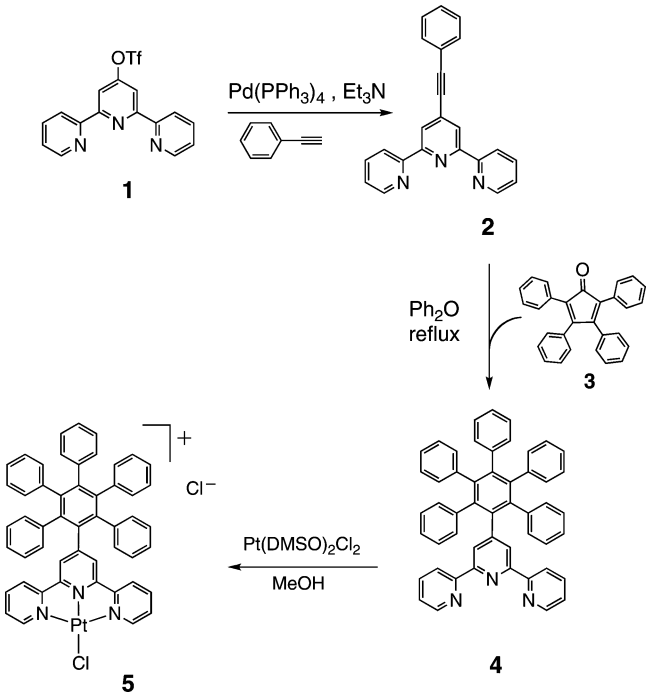

$2\sigma(I)$) and $wR2 = 0.2671$ (F^2, all data). There are very-large channels parallel to the *b* axis that contain methanol solvent molecules and chloride counterions. These areas are highly disordered to the extent that specific chloride sites could not be found from the difference Fourier map. Reflection contributions from species in the channels were removed using program *PLATON*, function *SQUEEZE*, which determined there to be a total of 2372 electrons in a volume of 7707 Å per unit cell removed (six channels per unit cell). The Cl^- counterions that were removed are accounted for in the chemical formula and calculations that derive therefrom. The data were very weak due to the high degree of disorder. This structural determination is intended for the demonstration of packing and to provide an estimate of intermolecular stacking distances.

Results and Discussion

Synthesis of New Compounds: Ligand TPPPB, 4, and Complex [Pt(TPPPB)Cl]Cl, 5. The synthetic sequence leading to the formation of the title complex **5** is outlined in Scheme 1 and commences with the formation of 4-(phenylethynyl)-2,2′:6′,2″-terpyridine through a Sonogoshira-catalyzed coupling using $Pd(PPh_3)_4$ and the subsequent reaction of that product with tetraphenylcyclopentadienone in refluxing diphenyl ether overnight by an yne−diene Diels−Alder reaction to give ligand **4**, which has been prepared previously by another procedure.[46] The insolubility of terpyridine derivative **1** in MeOH made its purification easy by continued washing of the solid until it became off-white in color. All of the reactions in the scheme involved no chromatography, making the procedure straightforward and time-saving for the synthesis of both ligand **4** and complex **5**. Whereas MeOH is a poor solvent for **4**, it was still used as the solvent for producing **5**, with the latter having unexpectedly better solubility. The reaction is finished when the suspension turns into a clear-orange solution, and the product (**5**) can be isolated by simple filtration followed by the addition of a large amount of ether into the flask to give a red precipitate denoted as **5-R** in >75% yield. As discussed later, it was also observed that a green solid-state form of the complex, denoted **5-G**, could be obtained upon exposure of **5-R** to vapors of methylene chloride and several other VOCs.

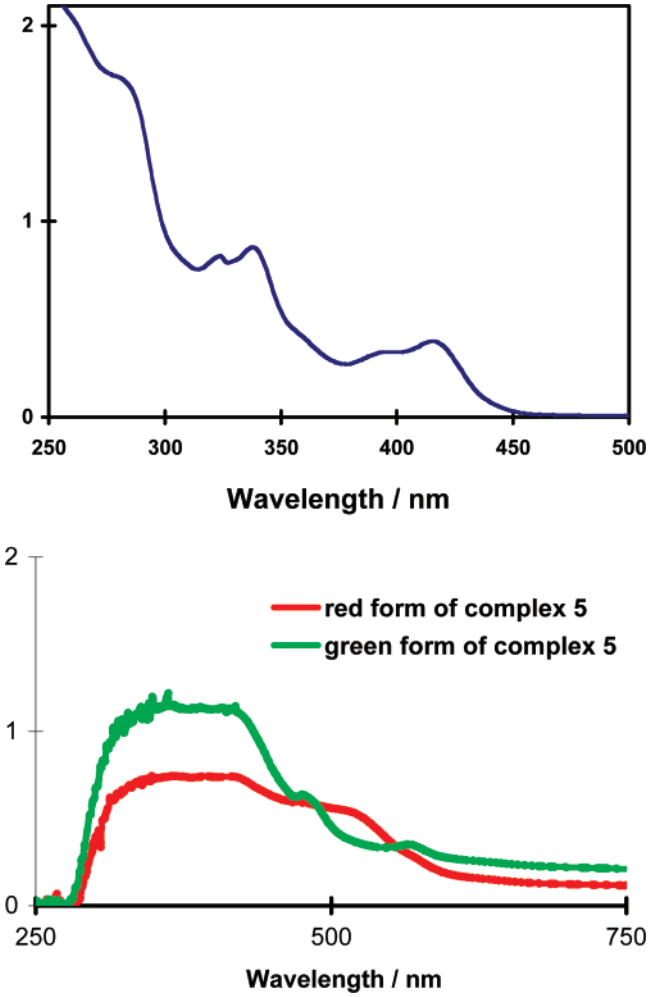

Figure 1. Top, absorption spectrum of **5** in CH_2Cl_2 (concentration: 5.0×10^{-5} M); bottom, diffuse reflectance spectra of **5-R** (red) and **5-G** (green) in the solid state at ambient room temperature.

5 is observed to be soluble, to differing extents, in a number of organic solvents including MeOH, CH_3CN, CH_2Cl_2, $CHCl_3$, DMF, and DMSO and was characterized by ^1H NMR, ^{13}C NMR, 2D-COSY, ESI-MS, and elemental analysis. The spectroscopic data are consistent with a cationic Pt(II) complex having a square-planar geometry with three of the four coordination sites occupied by the (pentaphenyl)-phenyl-modified terpyridyl ligand and the fourth site occupied by chloride.

Absorption and Emission Spectroscopy. The UV−vis absorption spectrum of **5** measured at room temperature in methylene chloride is shown in Figure 1. It exhibits a broad low-energy absorption between 370 and 460 nm with λ_{max} at 415 nm ($\epsilon = \sim 7740$ dm^3 mol^{-1} cm^{-1}), which corresponds to the $d\pi(Pt)-\pi(terpy)$ metal-to-ligand charge transfer (MLCT) transition based on previous assignments made for

(46) Ito, S.; Wehmeier, M.; Brand, D. J.; Kübel, C.; Epsch, R.; Rabe, J. P.; Müllen, K. *Chem.—Eur. J.* **2000**, *6*, 4327−4342.

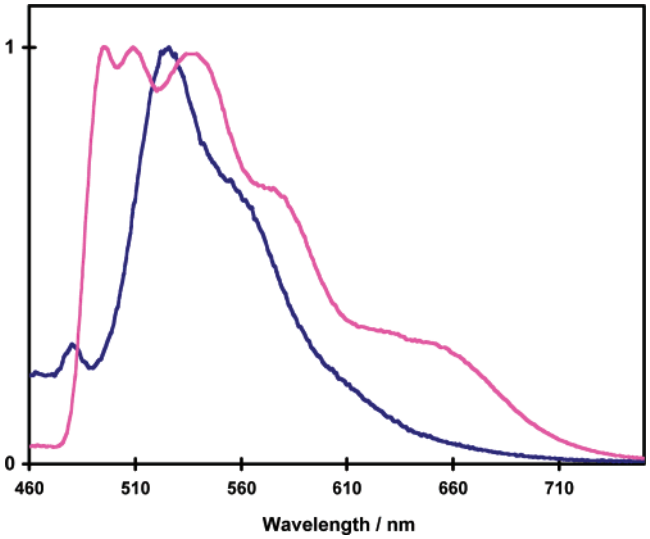

Figure 2. Emission spectrum of **5** at RT in CH_2Cl_2 (blue line, concentration: 1.0×10^{-5} M) and at 77 K in EtOH/MeOH (4:1) (red line, concentration: 1.0×10^{-5} M).

this class of complexes.[12,47−49] The absorption bands in the range of 280−370 nm correspond to spin-allowed intraligand ($\pi-\pi^*$) transitions ($\epsilon > 2 \times 10^4$ dm^3 mol^{-1} cm^{-1}) with maxima in the range of 335−340 nm. Also shown in Figure 1 are the diffuse reflectance spectra of the two solid-state forms of the complex, **5-R** and **5-G**, at ambient room temperature. The most-salient difference between these two spectra is the broad absorption of **5-R** that extends to nearly 600 nm, which accounts for the observed color difference.

Unlike [Pt(terpy)Cl]Cl,[12,50] **5** is emissive in solution at room temperature as shown in Figure 2, but its emission is not as intense as [Pt(ttpy)(C≡C-*p*-tol)]$^+$.[51,52] The emission spectrum was investigated further in methylene chloride at room temperature. When the complex is excited at 420 nm, the spectrum shows a broad emission band from 485 to 685 nm, with a maximum emission peak at 526 nm and a broad shoulder around 560 nm, giving a luminescence quantum yield (ϕ) of 0.0025 at λ_{em}^{max}, based on $[Ru(bpy)_3](PF_6)_2$ ($\phi = 0.062$).[53] On the basis of previous photophysical studies of closely related [Pt(terpyridyl)(acetylide)]$^+$ complexes, the excited state that gives rise to the observed emission is a triplet metal-to-ligand charge transfer (^{3}MLCT) involving a dπ metal orbital as the HOMO and a π^*(TPPPB) orbital as the LUMO. Upon cooling to 77 K in a 4:1 ethanol/methanol glass, the emission becomes much more intense (Figure 2). The structured emission between 475 and 750 nm contains multiple components with maxima at 496, 509, and 536 nm and also two shoulders at ca. 572 and 657 nm.

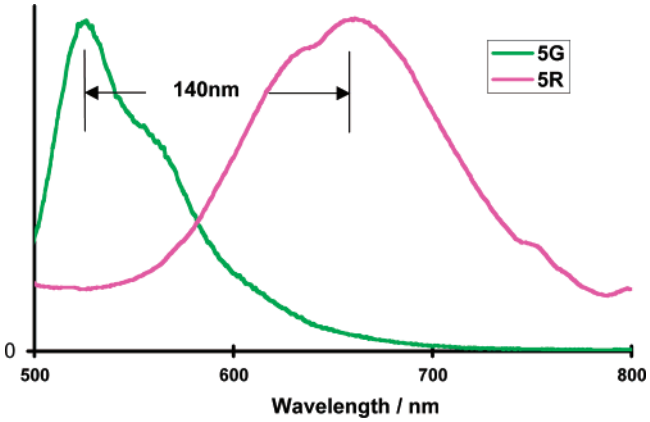

Figure 3. Emission spectra of **5-R** and **5-G** at 298 K in the solid state (4% in KBr).

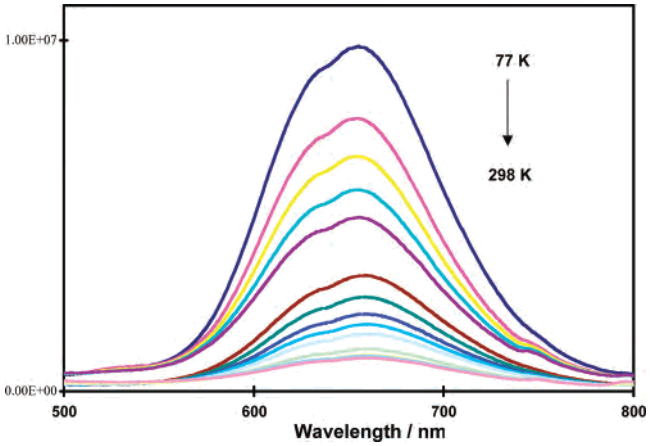

Figure 4. Emission spectra of **5-R** at different temperatures in the solid state (4% in KBr).

The two solid-state forms of **5** are brightly luminescent in the solid state at room temperature (RT) (Figure 3). Whereas the solid-state emission profile of **5-G** is similar to that of **5** in fluid solution, the emission spectrum of **5-R** is vastly different. The emission spectrum of **5-G** excited at 420 nm extends from 480 to 720 nm with a λ_{em}^{max} centered at 514 nm and two shoulders at ca. 550 and 591 nm that can be ascribed to vibronic structuring. On the other hand, excitation at 420 nm of a solid sample of **5-R** at RT leads to a broad emission centered at 654 nm, with a shoulder at 630 nm. The difference between emission maxima for **5-G** and **5-R** is substantial and can be attributed to a change in the charge-transfer excited state between the two forms, as discussed below. This difference also serves as the basis of the vapochromism of this complex.

When the temperature is lowered to 77 K, the energies of the emission maxima for both **5-R** and **5-G** remain unchanged, whereas the emission intensities increase approximately 10-fold for **5-R** and 12-fold for **5-G** as a result of lower rates of thermally activated nonradiative decay (Figures 4 and 5). The vibronic structuring in the spectrum of **5-G** becomes more pronounced at low temperatures, with

(47) Bailey, J. A.; Hill, M. G.; Marsh, R. E.; Miskowski, V. M.; Schaefer, W. P.; Gray, H. B. *Inorg. Chem.* **1995**, *34*, 4591−4599.
(48) Michalec, J. F.; Bejune, S. A.; Cuttell, D. G.; Summerton, G. C.; Gertenbach, J. A.; Field, J. S.; Haines, R. J.; McMillin, D. R. *Inorg. Chem.* **2001**, *40*, 2193−2200.
(49) Michalec, J. F.; Bejune, S. A.; McMillin, D. R. *Inorg. Chem.* **2000**, *39*, 2708−2709.
(50) Buchner, R.; Field, J. S.; Haines, R. J.; Cunningham, C. T.; McMillin, D. R. *Inorg. Chem.* **1997**, *36*, 3952−3956.
(51) Yang, Q.-Z.; Wu, L.-Z.; Wu, Z.-X.; Zhang, L.-P.; Tung, C.-H. *Inorg. Chem.* **2002**, *41*, 5653−5655.
(52) Du, P.; Schneider, J.; Jarosz, P.; Eisenberg, R. *J. Am. Chem. Soc.* **2006**, *128*, 7726−7727.
(53) Calvert, J. M.; Caspar, J. V.; Binstead, R. A.; Westmoreland, T. D.; Meyer, T. J. *J. Am. Chem. Soc.* **1982**, *104*, 6620−6627.

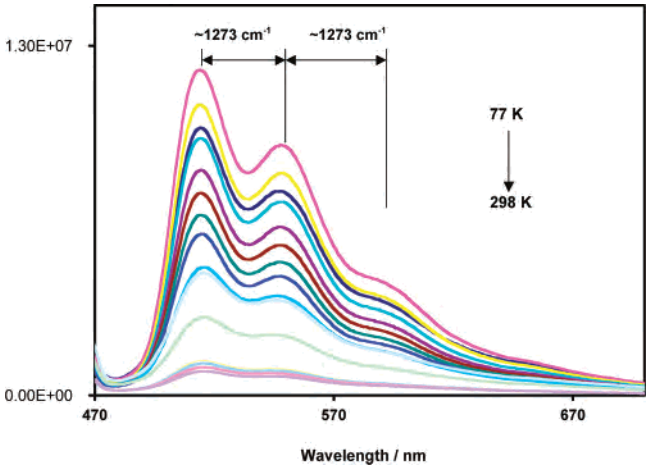

Figure 5. Emission spectra of **5-G** at different temperatures in the solid state (4% in KBr).

a separation between maxima of ca. 1273 cm^{-1}, corresponding to an aromatic vibrational mode of the terpyridyl ligands.[51,54]

The absence of a shift in the solid-state emission maxima of **5-R** and **5-G** upon lowering the temperature stands in contrast to what has been observed previously for related systems.[38,44,47,50] In [Pt(Nttpy)Cl],[38] a red-shift upon cooling of the solid-state sample was shown to correlate with lattice contraction and the decrease of the Pt···Pt separation, whereas a similar red-shift for [(RC^N^C)Pt] seen by Che and co-workers[44] was ascribed to excimeric $\pi\pi^*$ excited states and increasing interactions at low temperatures. The gold complex $\{Tl[Au(C_6Cl_5)_2]\}_n$[37] has also been reported to exhibit a shift to lower energy for the emission maximum when the temperature is lowered from 298 to 77 K, with the red-shift resulting from the shortened Au−Tl distance at low temperatures. In the present case, the absence of red-shifts in the emission energies for **5-R** and **5-G** as the temperature is lowered relates to the bulkiness and propeller-like nature of the pentaphenylphenyl moiety (vide infra) and the resultant inability of the cationic complexes to stack more tightly with reduced Pt···Pt distances.

Vapochromic Behavior of [Pt(TPPPB)Cl]Cl, 5. Vapochromism for **5** is seen upon the diffusion of methylene chloride into solid [Pt(TPPPB)Cl]Cl, as the original red color of the solid (**5-R**) changes to green (**5-G**). In going from **5-R** to **5-G**, the λ_{em}^{max} shifts from 654 to 514 nm, a difference of 140 nm, corresponding to the largest vapochromic response shift that, to our knowledge, has been seen in systems of this type with VOCs. The conversion of **5-R** to **5-G** is entirely reversible, and the response is relatively rapid. The time for the red-to-green color change upon exposure to dichloromethane vapor is less than 1 min, whereas the return to red emission after vapor exposure is stopped takes several minutes in air at ambient temperature.

The vapochromism of **5** appears to be relatively selective. The only other VOCs that evoked the response seen with dichloromethane are ethanol, acetonitrile, and ethyl acetate, although the response times for these VOCs was distinctly longer than that seen with CH_2Cl_2. The vapochromic response of **5-R** to each of these VOCs is shown in the Supporting Information. They are all similar to what is seen with dichloromethane in Figure 3 but with slight differences of emission maximum (496, 506, and 498 nm for EtOH, MeCN, and EtOAc, respectively) and modest differences in the degree of vibronic structuring in the spectrum of the resultant green form.

No detectable change of emission energy was found in the presence of benzene, toluene, *n*-hexane, acetone, hexane, diethyl ether, chloroform, petroleum ether, pentane, tetrahydrofuran, isopropyl alcohol, and methanol vapors. However, when dichloromethane was mixed with these solvents and **5-R** was brought into contact with the resultant vapors, conversion to **5-G** was observed, supporting the notion of great selectivity for the sorption of dichloromethane in the presence of other VOCs.

Crystal Structures of [Pt(TPPPB)Cl]Cl, 5. Crystal structures of both the red and green forms of **5** have been determined by X-ray diffraction, and crystallographic data for both **5-R** and **5-G** are given in Table 1. Crystals of **5-R** were obtained by slow diffusion of diethyl ether into a concentrated solution of the complex in methanol, whereas those of **5-G** were obtained by the slow evaporation of a dichloromethane solution of **5**. Because of poor diffracting ability, possibly as the result of the extensive solvent and anion disorder in the crystal, the structure determination of **5-R** is unsatisfactory for a detailed metrical analysis, but it does provide accurate connectivity and packing information

Table 1. Crystallographic, Data Collection, and Structure Refinement Parameters for Both Forms of [Pt(TPPPB)Cl]Cl (**5-G** and **5-R**)

form	green (**5**−**G**)	red (**5**−**R**)
formula	$[PtCl(Ph_5Ph\text{-}terpy)][Cl]\cdot CH_2Cl_2$	$[PtCl(Ph_5Ph\text{-}terpy)][Cl]\cdot xCH_3OH$
emperical formula	$C_{51}H_{35}Cl_2N_3Pt$	$C_{51}H_{35}Cl_2N_3Pt$
fw	955.81	955.81
T (K)	100.0(1)	100.0(1)
wavelength (Å)	0.71073	0.71073
cryst syst	monoclinic	monoclinic
space group	*C*2/*c*	*P*2/*n*
Z	12	24
a (Å)	13.366(3)	29.850(9)
b (Å)	45.731(10)	21.834(7)
c (Å)	24.151(5)	44.023(13)
α, β, γ (deg)	90, 103.167(3), 90	90, 93.795(4), 90
V (Å^3)	14 374(5)	28 628(15)
ρ_{calcd} (Mg/m^3)	1.325	1.331
μ (mm^{-1})	3.074	3.087
cryst size (mm^3)	0.50 × 0.08 × 0.02	0.28 × 0.12 × 0.04
F(000)	5688	11 376
2θ range (deg)	1.63 to 27.10	1.32 to 25.00
limiting indicies	$-17 \le h \le 17$ $-58 \le k \le 58$ $-30 \le l \le 30$	$-35 \le h \le 35$ $-25 \le k \le 25$ $-52 \le l \le 52$
no. of reflns collected	91 641	249 515
no. of data / rest / params	15 854 / 12 / 789	50 150 / 2 / 1399
GOF[a]	0.968	0.977
R1, *wR2* (F^2, $I > 2\sigma(I)$)[b]	0.0557, 0.1141	0.1026, 0.2334
R1, *wR2* (F^2, all data)[b]	0.1151, 0.1268	0.1991, 0.2671

[a] GOF = $S = [\sum w(F_o^2 - F_c^2)^2/(m - n)]^{1/2}$, where m = number of reflections and n = number of parameters. [b] $R1 = \sum||F_o| - |F_c||/\sum|F_o|$. $wR2 = [\sum w(F_o^2 - F_c^2)^2/\sum w(F_o^2)^2]^{1/2}$, where $w = 1/[\sigma^2(F_o)^2 + (aP) + bP]$ and $P = {}^1/_3 \max(0, F_o^2) + [{}^2/_3]\, F_c^2$.

(54) Yam, V. W.-W.; Tang, R. P.-L.; Wong, K. M.-C.; Cheung, K.-K. *Organometallics* **2001**, *20*, 4476−4482.

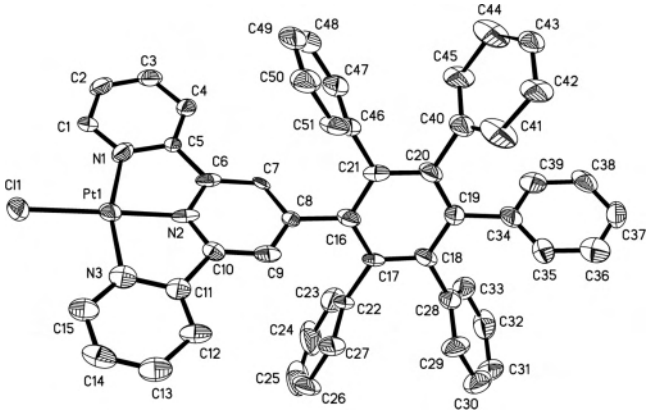

Figure 6. The structure of the $[PtCl(TPPPB)]^+$ cation in **5-G**.

as well as valid bond distances and angles involving the heavy atoms in the structure. Most importantly, Pt···Pt separations and the stacking of $[Pt(TPPPB)Cl]^+$ cations in **5-R** are accurately determined.

The molecular structure of cationic complex $[Pt(TPPPB)Cl]^+$ obtained from the determination of **5-G** is shown in Figure 6. The distortion in the square-planar geometry occasioned by the constraints of the terpyridyl ligand is evidenced by a N(1)−Pt−N(3) trans angle of 161.9(3)° and Pt−N distances that range from 1.900(7) to 2.031(7) Å, with the central nitrogen having the shortest distance. The Pt−Cl bond distance is 2.280(2) Å. The other bond distances and angles are similar to corresponding metrical parameters reported for other Pt(II) terpyridyl complexes.[38,54−57,58] Table 2 lists important bond lengths and angles for both the green (**5-G**) and red (**5-R**) crystalline forms.

Figure 7, which shows the packing arrangements for both **5-G** and **5-R**, reveals that, for **5-G**, the cationic Pt(II) complexes are stacked in a head-to-tail orientation, with two alternating distances between adjacent complexes. Despite perpendicular distances of 3.33 and 3.40 Å between neighboring terpyridyl ligands in **5-G**, the minimal direct overlap of terpyridyl carbon atoms when viewed down the stacking direction (part B of Figure 7) indicates small-to-negligible $\pi-\pi$ interactions, whereas the Pt···Pt distances of 3.9092(9) and 4.5483(11) Å and Pt···Pt···Pt angles of 153.4 and 167.5° give evidence of no significant metallophilic interactions in the crystal. The distances and nonlinearity of the cation stacking arrangement do not allow effective overlap of nearest-neighbor platinum d_{z^2} and p_z orbitals that are the basis of metallophilic interactions.[10,12,17,32,57,59−67] Solvent molecules of methylene chloride cannot be found in the crystal structure of **5-G**, but it is reasonable to assume that they reside in cavities between the stacks of the Pt(II) cationic complexes. The presence of methylene chloride has been confirmed in the ^{1}H NMR spectrum of dissolved crystals of **5-G** in DMSO-d_6 that shows ca. 0.7 molecules of methylene chloride per complex.

Table 2. Selected Bond Lengths (Angstroms) and Angles (Degrees) for Complex **5-G** and **5-R**

Form	5-G	5-R
Pt(1)−N(1)	2.031(7)	2.004(15)
Pt(1)−N(2)	1.900(7)	1.913(14)
Pt(1)−N(3)	2.024(7)	2.023(15)
Pt(1)−Cl(1)	2.280(2)	2.294(4)
N(2)−C(6)	1.374(10)	1.36(2)
N(3)−C(11)	1.387(10)	1.38(2)
N(3)−C(15)	1.350(10)	1.32(2)
N(1)−C(1)	1.299(9)	1.37(2)
N(1)−C(5)	1.355(9)	1.37(2)
C(1)−C(2)	1.390(11)	1.35(3)
C(8)−C(16)	1.514(10)	1.51(2)
C(5)−C(6)	1.473(10)	1.37(2)
C(10)−C(11)	1.500(11)	1.46(2)
C(6)−C(7)	1.401(10)	1.40(2)
C(9)−C(10)	1.355(10)	1.39(2)
C(11)−C(12)	1.352(11)	1.35(2)
N(1)−Pt(1)−N(2)	82.3(3)	80.4(6)
N(2)−Pt(1)−N(3)	79.6(3)	82.1(6)
N(1)−Pt(1)−N(3)	161.9(3)	162.4(6)
N(1)−Pt(1)−Cl(1)	98.6(2)	98.8(4)
N(2)−Pt(1)−Cl(1)	179.0(2)	177.5(5)
N(3)−Pt(1)−Cl(1)	99.5(2)	98.6(4)
C(1)−N(1)−C(5)	120.2(8)	118.6(16)
C(1)−N(1)−Pt(1)	126.5(6)	130.2(13)
C(6)−N(2)−Pt(1)	116.1(6)	118.1(11)
C(10)−N(2)−Pt(1)	122.5(6)	118.0(11)
C(11)−N(3)−Pt(1)	113.7(6)	111.9(12)
C(15)−N(3)−Pt(1)	127.4(6)	130.7(14)

The cationic packing of **5-R** is very different from that of **5-G**. As illustrated in part C of Figure 7, the stacking of the planar complexes in **5-R** has an irregular spiral arrangement, with each complex rotated by ca. 120° along the stacking direction. The structure is unusual in having six crystallographically independent complexes in the asymmetric unit, meaning that the asymmetric unit comprises two full turns along the stacking (helical) direction. Of the independent Pt···Pt separations, four are beyond the range considered indicative of metallophilic bonding but two are not. These short Pt···Pt separations are 3.30 and 3.34 Å, and the arrangement of the complexes containing these Pt(II) ions suggests that metallophilic bonding through d_{z^2} and p_z overlaps is occurring. Part D of Figure 7 shows a view of three complexes along the stacking direction − the first two have a short Pt···Pt separation with an eclipsing of the platinum atoms, whereas the third is displaced from the

(55) Yang, Q.-Z.; Tong, Q.-X.; Wu, L.-Z.; Wu, Z.-X.; Zhang, L.-P.; Tung, C.-H. *Eur. J. Inorg. Chem.* **2004**, 1948−1954.
(56) Yam, V. W.-W.; Tang, R. P.-L.; Wong, K. M.-C.; Ko, C.-C.; Cheung, K.-K. *Inorg. Chem.* **2001**, *40*, 571−574.
(57) Yam, V. W.-W.; Wong, K. M.-C.; Zhu, N.-Y. *J. Am. Chem. Soc.* **2002**, *124*, 6506−6507.
(58) Lai, S.-W.; Chan, M. C. W.; Cheung, K.-K.; Che, C.-M. *Inorg. Chem.* **1999**, *38*, 4262−4267.
(59) Roundhill, D. M.; Gray, H. B.; Che, C.-M. *Acc. Chem. Res. 22*, 55−61.
(60) Yip, H. K.; Che, C. M.; Zhou, Z. Y.; Mak, T. C. W. *J. Chem. Soc., Chem. Commun.* **1992**, 1369.
(61) Miskowski, V. M.; Houlding, V. H.; Che, C.-M.; Wang, Y. *Inorg. Chem.* **1993**, *32*, 2518−2524.
(62) Miskowski, V. M.; Houlding, V. H. *Inorg. Chem.* **1989**, *28*, 1529−1533.
(63) Biedermann, J.; Gliemann, G.; Klement, U.; Range, K. J.; Zabel, M. *Inorg. Chem.* **1990**, *31*, 4874.
(64) Bailey, J. A.; Miskowski, V. M.; Gray, H. B. *Inorg. Chem.* **1993**, *32*, 369−370.
(65) Chan, C.-W.; Lai, T. F.; Che, C.-M.; Peng, S.-M. *J. Am. Chem. Soc.* **1993**, *115*, 11245−11253.
(66) Liu, H. Q.; Peng, S. M.; Che, C.-M. *J. Chem. Soc., Chem. Comm.* **1995**, 509−510.
(67) Liu, H. Q.; Cheung, T. C.; Che, C.-M. *Chem. Comm.* **1996**, 1039−1040.

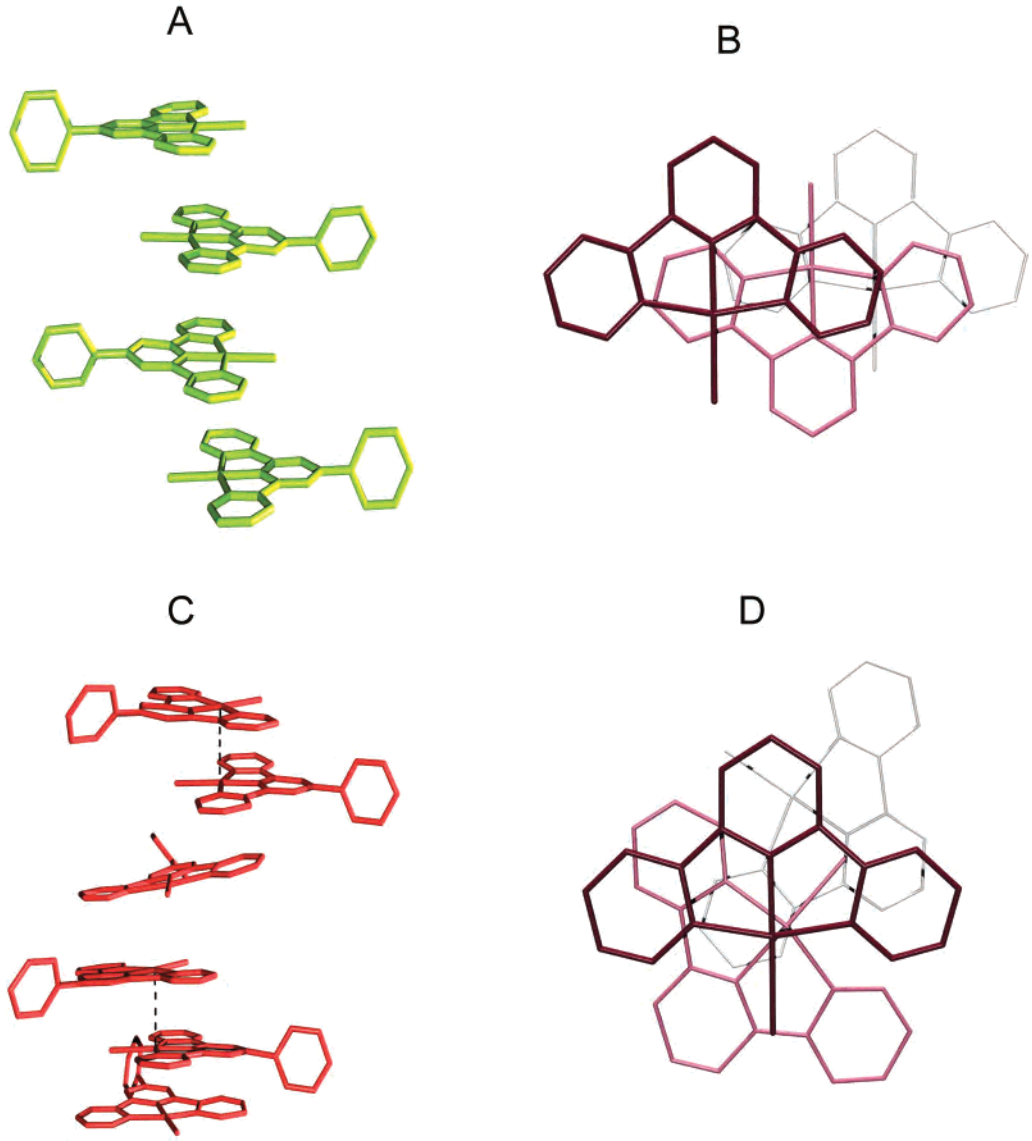

Figure 7. Comparison of the molecular stacking diagram in **5-G** (from side, **A**; from top, **B**) and **5-R** (from side, **C**; from top, **D**). Dashed lines show the Pt···Pt interactions in the **5-R** structure. The pentaphenyl substituents have been removed for clarity in the structure.

stacking direction and has no attractive interactions with neighboring complexes.

Basis of the Vapochromism of [Pt(TPPPB)Cl]Cl, 5. The structural and crystal packing data for the two solid-state forms of **5** provide a basis on which to interpret the observed vapochromic behavior. For some of the complexes in **5-R**, metallophilic interactions lead to a change in the nature of the HOMO and a consequent red-shift of the emission. Specifically, the HOMO for the metallophilicly interacting complexes is the σ^* combination of overlapping d_{z^2} orbitals and is thus delocalized over two platinum centers. The energy of this HOMO is greater than the energy of the d_{z^2} orbital in an isolated molecule of **5**, leading to a red-shift of the excited-state energy for the system. Because of the metal−metal nature of the HOMO, the emissive excited state in **5-R** is designated as ^{3}MMLCT.

Upon exposure to methylene chloride vapor, the packing arrangement and Pt···Pt interactions in **5-R** are disrupted with a consequent change in absorption and emission color. The structure of **5-G** shows that Pt···Pt interactions are essentially absent, leading to an excited-state emission that is essentially the same as that seen in fluid solutions of **5** − notably, ^{3}MLCT ($d\pi$(Pt)−π^*(TPPPB)) without perturbation from metallophilic interactions. It is interesting to note that in **5-R** some of the complexes do not exhibit Pt···Pt interactions, suggesting the possibility of a dual emission from both ^{3}MMLCT and ^{3}MLCT excited states from **5-R**. However, this is not the case, and a possible explanation is that rapid, efficient, and energetically favorable energy transfer occurs in **5-R** from ^{3}MLCT to ^{3}MMLCT, so that only the latter emission is observed.

Electrochemistry of [Pt(TPPPB)Cl]Cl, 5. A cyclic voltammogram of **5** is provided in the Supporting Information. The complex in DMF shows two reversible reduction waves at −0.59 and −1.18 V (estimated vs NHE using ferrocene as an internal standard with $E°(Fc^{+/0}) = +0.45$ V vs SCE[68] and SCE vs NHE = +0.24 V, with all of the scans done at 100 mV per second) and no oxidations within the solvent

(68) Connelly, N. G.; Geiger, W. E. *Chem. Rev.* **1996**, *96*, 877−910.

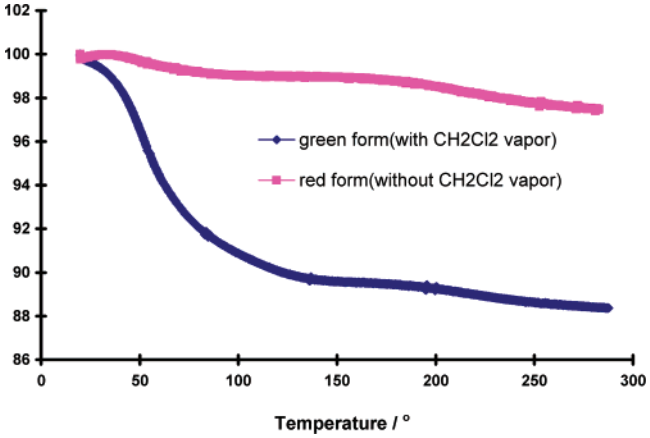

Figure 8. Thermogravimetric scans of **5-R** and **5-G**.

window. These results compare well with [Pt(tterpy)Cl]Cl on the reductive side, where two reversible waves are found at −0.59 and −1.13 V and are ascribed to two terpy ligand reductions. A similar assignment can be made for the reductions of **5**, with modest differences between the corresponding waves for **5** and [Pt(tterpy)Cl]Cl as the result of relatively minor electronic effects from the pentaphenylphenyl substituent in **5** to the *p*-tolyl group in [Pt(tterpy)Cl]Cl. The absence of an oxidation wave for **5** stands in contrast to an irreversible oxidation process seen for [Pt(tterpy)Cl]Cl around +1.60 V (vs NHE).

Thermogravimetric Study of the Vapochromic Process. The thermal stability of **5** and the loss of the VOC sorbed into it when vapochromism occurs was probed for dichloromethane by thermogravimetric analysis (Figure 8). The results indicate that, for **5-G**, approximately 9% of the mass is lost between 20 and 140 °C. Given that the molecular weight of **5** is 956, the lost mass corresponds to ∼86 amu, which would mean a stoichiometry of one molecule of dichloromethane per molecule of complex *if* all of the lost mass is assumed to be CH_2Cl_2. Independent assessment of the ratio of dichloromethane to complex was done by ^{1}H NMR spectroscopy using a sample of the X-ray quality crystals dissolved in DMSO-d_6. This experiment yielded a value of 0.7 for the dichloromethane/complex **5** ratio, which is reasonably consistent with the TGA results for **5-G**. A sample of **5-R** exhibits different TGA behavior, displaying only a very minor (<2%) mass loss up to approximately 300 °C.

Conclusions

The new vapochromic Pt(II) terpyridyl complex [Pt(TPPPB)Cl]Cl (**5**) has been synthesized, structurally characterized, and studied spectroscopically. The complex exhibits selective vapochromic behavior with VOCs including dichloromethane, acetonitrile, ethanol, and ethyl acetate. The magnitude of the vapochromic shift for this system is among the largest reported for simple VOCs, changing from red emission in the absence of selected VOCs to green in their presence. For dichloromethane, the response time to signal the presence of vapor through green emission is short (within seconds), whereas the return to the red form indicative of the absence of vapor occurs within a few minutes. The crystal structures of both the red and the green forms of **5**, the latter obtained upon recrystallization from CH_2Cl_2 solution, have been determined by X-ray diffraction studies, and analysis of the packing confirms that the red form **5-R** possesses significant Pt···Pt interactions with distances of 3.30 and 3.34 Å, whereas the green form **5-G** contains Pt(II) ions that are more-separated with Pt···Pt distances of 3.9092(9) and 4.5483(11) Å and Pt···Pt···Pt angles of 153.4 and 167.5°. The packing and spatial arrangements explain the distinct color changes between the two forms and their resultant photophysical properties. The green emission from **5-G** arises from a ^{3}MLCT excited state involving a HOMO of Pt(dπ) character and a LUMO localized on the terpyridyl ligand, whereas the red emission of **5-R** results from a ^{3}MMLCT charge-transfer excited state having the same LUMO but a different HOMO, as a consequence of metallophilic bonding. The vapochromic behavior is highly reversible and selective.

Acknowledgment. We wish to thank the Division of Basic Sciences, U.S. Department of Energy for financial support of this research (DE-FG02-90ER14125) and Dr. Chunchang Zhao and Prof. Man-Kit Ng for their help with the TGA measurements.

Supporting Information Available: Cyclic voltammograms of [Pt(TPPPB)Cl]Cl and [Pt(tterpy)Cl]Cl; characterization data of compounds **2**, **4** and **5** (LC-MS, ^{1}H NMR, ^{13}C NMR spectra and 2D COSY spectra of **5**); vapochromic response of compound **5-R** to ethanol, acetonitrile and ethyl acetate vapors. X-ray crystallographic data of [Pt(TPPPB)Cl]Cl as **5-R** and **5-G** is available in CIF format. This material is available free of charge via the Internet at http://pubs.acs.org.

IC700947G